Exchange functional by a range-separated exchange hole

Masayuki Toyoda* and Taisuke Ozaki

Research Center for Integrated Science (RCIS), Japan Advanced Institute of Science and Technology (JAIST), 1-1 Asahidai, Nomi, Ishikawa 923-1292, Japan

(Received 25 January 2011; published 29 March 2011)

An approximation to the exchange-hole density is proposed for the evaluation of the exact exchange energy in electronic structure calculations within the density-functional theory and the Kohn-Sham scheme. Based on the localized nature of density matrix, the exchange hole is divided into the short-range (SR) and long-range (LR) parts by using an adequate filter function, where the LR part is deduced by matching of moments with the exactly calculated SR counterpart, ensuring the correct asymptotic $-1/r$ behavior of the exchange potential. With this division, the time-consuming integration is truncated at a certain interaction range, largely reducing the computation cost. The total energies, exchange energies, exchange potentials, and eigenvalues of the highest-occupied orbitals are calculated for the noble-gas atoms. The close agreement of the results with the exact values suggests the validity of the approximation.

DOI: 10.1103/PhysRevA.83.032515 PACS number(s): 31.15.eg

I. INTRODUCTION

The density-functional theory [1] in the formulation by Kohn, Sham, and Levy [2,3] (KS-DFT) is a methodology that is now recognized as one of the most powerful tools to investigate the electronic structures of atoms, molecules, and solids. The high computational efficiency is afforded by transforming the problem of interacting electrons to a single-body problem of noninteracting electrons placed in an effective potential. Therefore, the central problem lies in the way in which to describe the electronic exchange and correlation by the effective potential. The local-density approximation (LDA) [2] describes it as a local potential that is derived from the exchange and correlation energy of a uniform electron gas. In the generalized gradient approximation (GGA) [4–6], a semilocal potential is used where the electronic density gradient is also taken into account. The local and semilocal effective potentials provide a well-balanced compromise between reliability and feasibility and are, thus, used routinely in the fields of quantum chemistry, solid-state physics, and biophysics.

The KS-DFT methods with LDA and GGA are, however, also known for systematic errors such as the significant underestimation of the band-gap energy of semiconductors and insulators. The failure of the semilocal approximation is manifested by the incomplete cancellation of the self-Hartree energy for each orbital, known as the self-interaction error (SIE), and the incorrect asymptotic decay of the exchange-correlation potential. Since it is primarily caused by the poor description of the exchange interaction, the error is remedied by using the exact exchange (EXX). There have been several such approaches, including the hybrid functional methods [7–10] where a fraction (typically, $\sim 1/4$) of EXX are admixed with the semilocal exchange and the range-separated exchange methods [11–14], where either the short-range (SR) or long-range (LR) part of EXX is combined with the semilocal counterpart.

The high computation cost required for the evaluation of EXX is an obvious drawback of the hybrid methods. The scaling of the computation in the canonical way is $O(N^4)$, where N is a measure of the system size. Although it can be reduced to $O(N^2)$ in a local-basis implementation [15], it is still higher than the $O(N)$ scaling of the semilocal exchange. A further reduction of the scaling may be attained by modifying the exchange interaction into the *screened* exchange interaction by multiplying an exponentially decaying factor to the Coulomb operator. Among the above-mentioned methods, this approach is employed in the screened hybrid functional method [10] and the screened-exchange LDA method [12,14]. Not only being advantageous in terms of computation time, this technique is as well found to mimic a part of the correlation effects by screening out the LR part of exchange and to improve the results for several quantities in metals and semiconductors. However, the other groups [13,16–18] take the opposite approach where the LR part of EXX [or the exchange-correlation calculated by a post Hartree-Fock (HF) method] is combined with the SR part of a semilocal exchange correlation, claiming the importance of the LR asymptotic tail of the exchange potential. A way to somehow recover the correct $-1/r$ tail of the screened-exchange potential, therefore, seems to be advantageous in both the physical and computational points of view.

In this paper, a scheme to calculate EXX is proposed with our goal to achieve high computational efficiency comparable to the computation of the semilocal exchange. Although the idea of the range-separated exchange is utilized, neither the SR nor LR part is screened out. The fundamental idea behind the presented scheme is the general nature of electrons in materials that the electronic structure is much less sensitive to a change of an external potential in a far-away region. This principle is known as *nearsightedness* [19], forming the basis of linear-scaling DFT methods [20]. Our ansatz is as follows: the SR part of the exchange potential possesses most of the physical significance and, thus, the LR part is easily estimated by referring the SR counterpart. This idea may enable us to develop an exchange functional for KS-DFT calculations where the exact properties of EXX are fulfilled, such as the cancellation of SIE and the correct asymptotic behavior of the exchange potential, with $O(N)$ computation cost. This paper

*m-toyoda@jaist.ac.jp

is organized as follows. In Sec. II, the detailed formulation of the scheme is presented. In Sec. III, the computation results for noble-gas atoms are shown and the manner in which the ansatz works for atomic systems is discussed. Finally, a summary is given in Sec. IV.

II. FORMULATION

A. Exchange energy

In KS-DFT, EXX for a spin channel is given, in atomic units ($\hbar = m_e = e^2 = 1$), as follows:

$$E_X = -\frac{1}{2}\sum_{i,j}^{\mathrm{occ}} \int\int \frac{\psi_i^*(\boldsymbol{r})\psi_j^*(\boldsymbol{r}')\psi_j(\boldsymbol{r})\psi_i(\boldsymbol{r}')}{|\boldsymbol{r}-\boldsymbol{r}'|} d^3r\, d^3r', \quad (1)$$

where $\psi_i(\boldsymbol{r})$ is the ith KS orbital and the summation is taken over all the occupied orbitals. This is not an explicit functional of the total charge density $\rho(\boldsymbol{r})$ but of the first-order reduced density matrix (1-RDM)

$$\gamma(\boldsymbol{r},\boldsymbol{r}') = \sum_{i}^{\mathrm{occ}} \psi_i^*(\boldsymbol{r})\psi_i(\boldsymbol{r}'). \quad (2)$$

The exchange energy (1) is also expressible in the following form:

$$E_X = -\frac{1}{2}\int\int \frac{\rho(\boldsymbol{r})\rho_X(\boldsymbol{r},\boldsymbol{r}')}{|\boldsymbol{r}-\boldsymbol{r}'|} d^3r\, d^3r', \quad (3)$$

where $\rho_X(\boldsymbol{r},\boldsymbol{r}')$ is the exchange hole density

$$\rho_X(\boldsymbol{r},\boldsymbol{r}') = \frac{|\gamma(\boldsymbol{r},\boldsymbol{r}')|^2}{\rho(\boldsymbol{r})}. \quad (4)$$

As in the case of the range-separated exchange methods, the exchange hole is divided into the SR and LR parts as follows:

$$\rho_X(\boldsymbol{r},\boldsymbol{r}') = D(s)\rho_X(\boldsymbol{r},\boldsymbol{r}') + [1-D(s)]\rho_X(\boldsymbol{r},\boldsymbol{r}'), \quad (5)$$

where $D(s)$ is a function of $s = |\boldsymbol{r}-\boldsymbol{r}'|$, which is unity at $s = 0$ and decreases rapidly (exponentially, in general) as s increases, approaching to zero at $s \to \infty$. Therefore, the first and second terms of the right-hand side (r.h.s.) in Eq. (5) correspond to the SR and LR parts of the exchange hole, respectively.

Here, we estimate the LR part by referring the SR part. A qualitative support to this idea is given by the fact that the 1-RDM in materials shows rapid decay as $\gamma \propto \exp(-\lambda s)$, where the exponent is $\lambda \propto E_g$ (small gap) or $\lambda \propto \sqrt{E_g}$ (large gap) in an insulator with direct gap energy E_g, and $\lambda \propto T$ (low temperature) or $\lambda \propto \sqrt{T}$ (high temperature) in a metal with electronic temperature T [21,22]. Under this idea, the LR part is replaced by an analytic function $f(\{\alpha(\boldsymbol{r})\};s)$ that models the spherically averaged exchange hole where $\alpha(\boldsymbol{r}) = (a(\boldsymbol{r}),b(\boldsymbol{r}),\dots)$ is a composite parameter determined self-consistently at each point of $\boldsymbol{r}$ in space. Note that the spherical average does not lack mathematical rigor because of the isotropic nature of the Coulomb interaction. Our exchange hole is, therefore,

$$\tilde{\rho}_X(\boldsymbol{r},\boldsymbol{r}') = D(s)\rho_X(\boldsymbol{r},\boldsymbol{r}') + [1-D(s)]f(\{\alpha(\boldsymbol{r})\};s), \quad (6)$$

which should fulfill the conditions that an exact exchange hole does, such as the non-negativity and the unit normalization

$$4\pi\int_0^\infty \tilde{\rho}_X(\boldsymbol{r},\boldsymbol{r}')\, d^3r' = 1. \quad (7)$$

By substituting Eq. (6) in Eq. (3), the exchange energy is given as

$$\tilde{E}_X = -\frac{1}{2}\int\int^{s<s_{\max}} \frac{D(s)}{s}\rho(\boldsymbol{r})\rho_X(\boldsymbol{r},\boldsymbol{r}')d^3r\, d^3r' - \frac{1}{2}\int \rho(\boldsymbol{r})\tilde{\epsilon}_X^{\mathrm{LR}}(\boldsymbol{r})\, d^3r, \quad (8)$$

where

$$\tilde{\epsilon}_X^{\mathrm{LR}}(\boldsymbol{r}) = 4\pi\int_0^\infty \frac{1-D(s)}{s} f(\{\alpha(\boldsymbol{r})\};s)s^2\, ds. \quad (9)$$

The decaying function $D(s)$ in Eq. (8) enables one to terminate the numerical integration at a finite interaction length $s_{\max}$, which reduces the scaling of the computation.

So far, the scheme is introduced without defining the decaying function $D(s)$ and the model exchange-hole function $f(\{\alpha\};s)$. In the preceding works, two types of decaying functions have been used. One is the Thomas-Fermi- (TF-) type screening function [11]

$$D^{\mathrm{TF}}(s) = \exp(-k_s s), \quad (10)$$

where k_s is the Thomas-Fermi wave vector [23]. This is of the same shape as Yukawa's short-range nuclear force. The other type is called the erf screening [16]:

$$D^{\mathrm{erf}}(s) = \mathrm{erfc}(\mu s) \equiv \frac{2}{\sqrt{\pi}}\int_{\mu s}^\infty e^{-t^2} dt. \quad (11)$$

As a variation of the erf screening, Toulouse *et al.* have recently proposed another function called erfgau interaction [17]. As the first test, we choose $D^{\mathrm{erf}}(s)$ for our decaying function. The parameter μ determines the range in which the SR and LR parts are separated. For the model exchange hole, the following form is used:

$$f_H(a,b,s) = \frac{a}{16\pi bs}[(a|b-s|+1)\exp(-a|b-s|) - (a|b+s|+1)\exp(-a|b+s|)]. \quad (12)$$

This is analytically derived from the $1s$ wave function of a hydrogenic atom and was previously used by Becke and Roussel [24] to describe the exchange hole in a meta-GGA method. By construction, the function (12) satisfies the exact conditions for an exchange hole: it has always a non-negative value and the norm is unity throughout its domain ($a \geqslant 0$, $b \geqslant 0$, and $s \geqslant 0$). With the choice, the exchange energy [Eq. (3)] and the LR energy density [Eq. (9)] have the following explicit forms:

$$\tilde{E}_X = -\frac{1}{2}\int\int^{s<s_{\max}} \frac{\mathrm{erfc}(\mu s)}{s}\rho(\boldsymbol{r})\rho_X(\boldsymbol{r},\boldsymbol{r}')\, d^3r\, d^3r' - \frac{1}{2}\int \rho(\boldsymbol{r})\tilde{\epsilon}_X^{\mathrm{LR}}(a(\boldsymbol{r}),b(\boldsymbol{r});\mu)\, d^3r, \quad (13)$$

and

$$\tilde{\epsilon}_X^{\mathrm{LR}}(x,y;\mu) = \mu\left\{\frac{\mathrm{erf}(y)}{2y} + \frac{e^{x^2}}{4y} + [(x^2-1-xy)\,\mathrm{erfc}(x-y)\,e^{-xy} - (x^2-1+xy)\,\mathrm{erfc}(x+y)\,e^{xy}]\right\}, \quad (14)$$

respectively, where $x = a/2\mu$ and $y = b\mu$.

B. Parameter determination

The model parameters a and b are determined by matching moments of the exchange hole. The nth moment of the exactly calculated SR part is

$$M_n(\boldsymbol{r}) \equiv 4\pi \int_0^{s_{\max}} D(s)\rho_X(\boldsymbol{r},s)s^{2-n}ds, \quad (15)$$

while that of the corresponding SR part of the model exchange hole is

$$\mu_n(a,b) \equiv 4\pi \int_0^{\infty} D(s) f_H(a,b;s)s^{2-n}ds. \quad (16)$$

The conditions appropriate for determination of the parameters might be

$$M_0(\boldsymbol{r}) = \mu_0(a,b) \quad (17)$$

and

$$M_1(\boldsymbol{r}) = \mu_1(a,b), \quad (18)$$

which physically mean the normalization of the hole (7) and the agreement of the SR exchange potential, respectively. The conditions (17) and (18) must and can be met simultaneously if the model function has enough flexibility to reproduce the exact hole. In practice, however, there is no guarantee for the existence of a and b that satisfies both the requirements for a given model function. In fact, with Eq. (12), we found it impossible to find a and b to satisfy both requirements simultaneously for a certain range of values of $M_0(\boldsymbol{r})$ and $M_1(\boldsymbol{r})$. Therefore, we search a and b, which give μ_1 most close to M_1 instead of the condition (18), while keeping the other condition (17) satisfied. This search is achieved by using the Lagrange multipliers. The Lagrangian is

$$\mathcal{L}(a,b) = [\Delta_1(a,b)]^2 + \lambda\Delta_0(a,b) + P(b), \quad (19)$$

where Δ_n is the relative difference between the exact moment and the model moment

$$\Delta_n(a,b) = \mu_n(a,b)/M_n(\boldsymbol{r}) - 1, \quad (20)$$

and

$$P(b) = \begin{cases} P_0(b-b_{\min})^6 & b < b_{\min}, \\ 0 & b \geqslant b_{\min} \end{cases} \quad (21)$$

is a penalty function, with an arbitrary constant P_0, which is introduced to prevent b from being too small due to a technical reason that some of the analytic expressions such as Eq. (14) become numerically unstable when b approaches to zero. At the stationary point of $\mathcal{L}$, three conditions are obtained by differentiating $\mathcal{L}$ with respect to a, b, and λ. One of them is, of course, the condition (17). By erasing λ from the remaining two conditions, the following condition is obtained:

$$2\Delta_1 D + \frac{dP}{db}\frac{\partial\Delta_0}{\partial a} = 0, \quad (22)$$

where

$$D \equiv \frac{\partial\Delta_0}{\partial a}\frac{\partial\Delta_1}{\partial b} - \frac{\partial\Delta_1}{\partial a}\frac{\partial\Delta_0}{\partial b}. \quad (23)$$

For a fixed value of a, the model function (12) is a monotonic function of b. It is thus easy to find b, which satisfies the requirement (17) for given a by using a simple search algorithm such as the bisection search. Then, since now b can be treated as a bound variable, it is also straightforward to find a, which satisfies the remaining requirement (22). Therefore, the determination process is a tractable task.

Computation of the moments is also not time consuming for the following reason: Calculating M_n over the whole space is computationally similar to taking an integral over $\boldsymbol{r}$ of Eq. (15), which leads to almost the same expression as the first term of Eq. (8). Therefore, it can be performed by applying conventional techniques for calculating EXX, for example, by calculating the electron-repulsion integrals of the Gaussian basis set [25] or of a numerically defined localized basis set [15]. The computation is actually not heavier than the calculation of the energy (8) itself.

C. Derivatives

The effective potential for the KS equations that corresponds to the exchange energy (13) is obtained by taking the functional derivatives with respect to variations of the KS orbitals. The functional derivatives in the present scheme are well defined except for the model parameters a and b. Since they have to be optimized numerically, there is no analytic relation between the parameters and the orbital wave functions. However, since the conditions (17) and (22) are assumed to be rigorously satisfied, the conditions must also be stationary against the variations and, thus, the following equations are obtained:

$$\delta(\Delta_0) = 0, \quad (24)$$

$$\delta\left(2\Delta_1 D + \frac{dP}{db}\frac{\partial\Delta_0}{\partial a}\right) = 0. \quad (25)$$

They are arranged in the following algebraic representation:

$$A\begin{pmatrix}\delta a\\ \delta b\end{pmatrix} = B\begin{pmatrix}\delta M_0\\ \delta M_1\end{pmatrix}, \quad (26)$$

where A and B are 2×2 matrices with the matrix elements

$$a_{00} = \frac{\partial\Delta_0}{\partial a}, \quad (27)$$

$$a_{01} = \frac{\partial\Delta_0}{\partial b}, \quad (28)$$

$$a_{10} = 2D\frac{\partial\Delta_1}{\partial a} + 2\Delta_1\frac{\partial D}{\partial a} + \frac{dP}{db}\frac{\partial^2\Delta_0}{\partial a^2}, \quad (29)$$

$$a_{11} = 2D\frac{\partial\Delta_1}{\partial b} + 2\Delta_1\frac{\partial D}{\partial b} + \frac{dP}{db}\frac{\partial^2\Delta_0}{\partial a\partial b} + \frac{d^2P}{db^2}\frac{\partial\Delta_0}{\partial a}, \quad (30)$$

$$b_{00} = (\Delta_0+1)/M_0, \quad (31)$$

$$b_{11} = 2D(2\Delta_1+1)/M_1, \quad (32)$$

and $b_{01} = b_{10} = 0$. Since the variation of M_0 and M_1 is well defined, the variation of the parameters can be analytically obtained as follows:

$$\begin{pmatrix} \delta a \\ \delta b \end{pmatrix} = A^{-1} B \begin{pmatrix} \delta M_0 \\ \delta M_1 \end{pmatrix}. \tag{33}$$

Finally, the functional derivative of Eq. (13) is explicitly given as

$$\frac{\delta \tilde{E}_X}{\delta \psi_i^*(\boldsymbol{r})} = -\sum_j^{\text{occ}} \psi_j(\boldsymbol{r}) \int^{s<s_{\max}} \tilde{v}(\boldsymbol{r},s)\psi_i(\boldsymbol{r}')\psi_j^*(\boldsymbol{r}')\, d^3r' - \frac{1}{2}\psi_i(\boldsymbol{r})\left[\tilde{\epsilon}_X^{\text{LR}}(\boldsymbol{r}) - \alpha M_0(\boldsymbol{r}) - \beta M_1(\boldsymbol{r})\right], \tag{34}$$

where

$$\alpha \equiv \frac{\partial \tilde{\epsilon}_X^{\text{LR}}}{\partial a} c_{00} + \frac{\partial \tilde{\epsilon}_X^{\text{LR}}}{\partial b} c_{10}, \tag{35}$$

$$\beta \equiv \frac{\partial \tilde{\epsilon}_X^{\text{LR}}}{\partial a} c_{01} + \frac{\partial \tilde{\epsilon}_X^{\text{LR}}}{\partial b} c_{11}, \tag{36}$$

and c_{ij} is the matrix element of $C = A^{-1}B$. The first term of the r.h.s. in Eq. (34) is a Hartree-Fock-type nonlocal potential and, thus, is dealt with by the Fock matrix of the Roothann equation in terms of a basis set expansion where the Coulomb operator is replaced with

$$\tilde{v}(\boldsymbol{r},s) \equiv D(s)\left(\frac{1+\beta}{s} + \alpha\right). \tag{37}$$

The second term is a semilocal potential and is treated in the same way as the LDA potential.

The derivatives with respect to the atomic nuclear positions are often required to calculate the force acting on the atoms for molecular dynamic simulations. The derivatives are also analytically obtained by using the relation of Eq. (33).

D. Self-exchange energy

The importance of using EXX lies mainly in the fact that the self-exchange energy for each KS orbital exactly cancels the corresponding self-Hartree energy. In this scheme, the exchange energy for i-th orbital is

$$\langle \psi_i | \hat{V}_X | \psi_i \rangle = -\sum_j^{\text{occ}} \left\langle \psi_i \psi_j \left| \frac{D(s)}{s} \right| \psi_j \psi_i \right\rangle - \frac{1}{2}\int \rho_i(\boldsymbol{r}) \tilde{\epsilon}_X^{\text{LR}}(\boldsymbol{r}) + \iint d^3r\, d^3r'\, D(s)\left(\alpha(\boldsymbol{r}) + \frac{\beta(\boldsymbol{r})}{s}\right)\gamma(\boldsymbol{r}',\boldsymbol{r}) \times \left[\frac{\rho_i(\boldsymbol{r})}{\rho(\boldsymbol{r})}\gamma(\boldsymbol{r},\boldsymbol{r}') - \psi_i^*(\boldsymbol{r})\psi_i(\boldsymbol{r}')\right], \tag{38}$$

where $\rho_i(\boldsymbol{r}) = \psi_i^*(\boldsymbol{r})\psi_i(\boldsymbol{r})$ is the orbital charge density. This includes both the self- and mutual-exchange energy. In the sum in the first term, the $i = j$ term describes the SR part of the self-exchange energy while the other $i \neq j$ terms are the SR part of the mutual-exchange energy. In the second term, the separation of the self-exchange from the mutual-exchange is not clear. The remaining term is characterized by the factor

$$\frac{\rho_i(\boldsymbol{r})}{\rho(\boldsymbol{r})}\gamma(\boldsymbol{r},\boldsymbol{r}') - \psi_i^*(\boldsymbol{r})\psi_i(\boldsymbol{r}'), \tag{39}$$

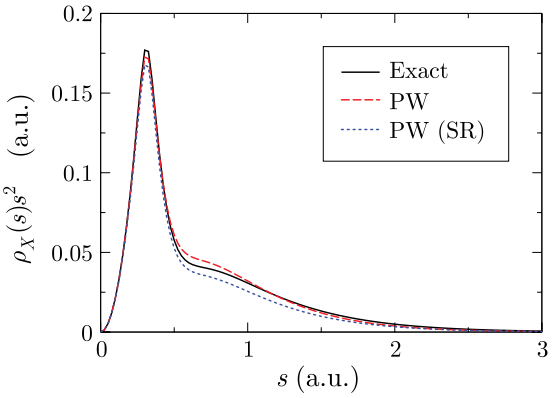

FIG. 1. (Color online) Exchange hole of a neon atom at $r = 0.31$ a.u. The exact hole function (solid line), the hole in the present scheme (dashed line) with the parameter $\mu = 0.1$ a.u.$^{-1}$, and the SR part of the hole in the present scheme (dotted line) are plotted after multiplied by s^2.

which is the difference between the nonlocal orbital density and 1-RDM weighted by the orbital density. It vanishes after taking summation over orbitals. In one-electron systems, such as a hydrogen atom, the first and second terms are the *correct* self-exchange energy and the third term vanishes. For many electron-systems, although the first term correctly cancels the SR part of the self-Hartree energy, the second term might include the LR part of the self-exchange energy and the third term does not vanish. However, since SIE is significant for a localized orbital and the difference (39) is small when $\boldsymbol{r}$ and $\boldsymbol{r}'$ are close to each other, it is expected that the LR part of the self-exchange and the difference (39) can be negligible and therefore that SIE is nearly completely canceled in this method.

III. CALCULATION

The presented method has been implemented in our in-house program for electronic structure calculations of atomic systems based on the real-space finite-element method [26]. The advantage of the program is that all the integrations are performed analytically except for those for the

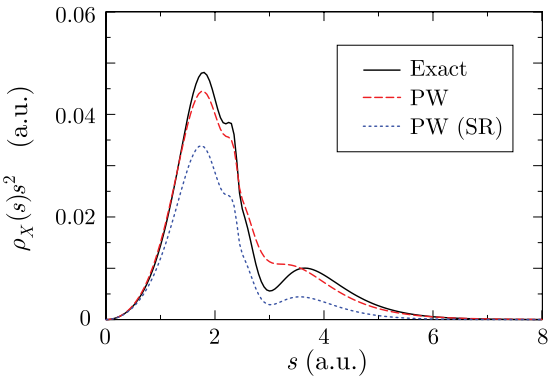

FIG. 2. (Color online) Exchange hole of an argon atom at $r = 2.48$ a.u. The exact hole function (solid line), the hole in the present scheme (dashed line) with the parameter $\mu = 0.1$ a.u.$^{-1}$, and the SR part of the hole in the present scheme (dotted line) are plotted after multiplied by s^2.

TABLE I. Comparison of the exchange energy E_X (in hartree), calculated in various exchange functionals for the noble-gas atoms. The orbitals are calculated by the HF method.

				PW[a]				
	Exact	LDA	GGA [5]	$\mu = 0.1$	$\mu = 0.2$	$\mu = 0.3$	$\mu = 0.4$	$\mu = 0.5$
He	−1.0258	−0.884	−1.025	−1.0258	−1.0258	−1.0259	−1.0261	−1.0263
Ne	−12.1084	−11.03	−12.14	−12.1084	−12.1092	−12.1113	−12.1149	−12.1200
Ar	−30.1849	−27.86	−30.15	−30.1851	−30.1869	−30.1915	−30.1990	−30.2083
Kr	−93.8560	−88.62	−93.87	−93.8563	−93.8596	−93.8680	−93.8815	−93.8986
Xe	−179.0971	−170.6	−179.0	−179.0976	−179.1029	−179.1155	−179.1349	−179.1596
Rn	−387.5037	−373.0	−387.5	−387.5045	−387.5117	−387.5290	−387.5559	−387.5913
AARE[b] (%)		7	0.09	0.0002	0.0004	0.01	0.03	0.05

[a]This work with various values of μ (in a.u.$^{-1}$).
[b]Average of absolute relative error.

exchange-correlation energy. For the exchange-correlation energy, the integration is performed by interpolating the charge density and the exchange-correlation potential with a set of finite-element basis functions. Therefore, the numerical error is determined solely by the interval of the radial grid points. In the following results, we have confirmed the convergence of the energy at least to the number of digits shown in the tables. The deviations from the exact values are thus directly attributed to the approximation of the presented method.

In Fig. 1, the exchange-hole density of a neon atom is plotted around a reference point at $r = 0.31$ a.u. away from the nucleus. The profile consists of a sharp peak from the core electrons and a broad feature from the valence electrons. The exchange hole in this method [Eq. (6)] is plotted by the dashed line where the separation parameter is chosen to be $\mu = 0.1$ a.u.$^{-1}$. The dotted line shows the SR part of the hole. It is clearly shown that the exact hole is localized within $s < 2$ a.u. and thus described well almost only by the SR part. In Fig. 2, the exchange-hole density of an argon atom is plotted around a reference point at $r = 2.48$ a.u. away from the nucleus. In this case, the profile becomes more complicated, reflecting the atomic shell structure. Although the shape is rather smeared out [27], the three dominant peaks are still well captured by this method.

In Table I, the exchange energy of the noble-gas atoms calculated by the present method with various values of the parameter μ are summarized and compared with the LDA, GGA, and exact results. All the energies are calculated with the exact wave function obtained by the HF calculations. The average absolute relative errors (AARE) from the exact values are listed in the bottom line. The values obtained by the present work (PW) are arranged in columns with different values of μ. For smaller values of μ, the presented method yields quite accurate exchange energies with error in order of 1 mili-hartree or even less than that. The error systematically increases as μ increases. With $\mu = 0.5$ a.u.$^{-1}$, the error is almost in the same order as the GGA results. Note that the GGA exchange energy is also acceptably accurate because the enhancement factor was often constructed to reproduce the exact exchange energy of the noble-gas atoms. The problem of the GGA exchange is actually in the description of the potential. Since the presented method can also yield an accurate potential as shown later, even the method with $\mu = 0.5$ a.u.$^{-1}$ performs much better than GGA.

In Table II, the total energy of the noble-gas atoms in the exchange-only calculations is summarized and compared with the values calculated with the optimized effective potentials (OEP) [30,31], as well as the exact value by the HF method. The OEP method has been used to evaluate EXX in the KS-DFT method with a local effective potential. Although it has been shown that the exact local exchange potential does not exist for the ground state of typical atoms [32], the OEP

TABLE II. Comparison of the total energy E (in hartree), calculated in various exchange-only approximations for the noble-gas atoms. The one-particle orbitals are self-consistently determined for within each approximation. Two sets of values obtained by the OEP method are shown for comparison where the OEP equations are solved numerically [28] or by using the Krieger-Li-Iafrate (KLI) approximaion [29], respectively.

				PW[a]				
	Exact	OEP [28]	KLI-OEP [29]	$\mu = 0.1$	$\mu = 0.2$	$\mu = 0.3$	$\mu = 0.4$	$\mu = 0.5$
He	−2.8617	−2.8617		−2.8616	−2.8616	−2.8617	−2.8618	−2.8619
Ne	−128.5471	−128.5454	−128.5449	−128.5471	−128.5480	−128.5498	−128.5531	−128.5580
Ar	−526.8175	−526.8122	−526.8105	−526.8177	−526.8193	−526.8236	−526.8308	−526.8399
Kr	−2752.0549	−2752.0430	−2752.0398	−2752.0552	−2752.0584	−2752.0663	−2752.0793	−2752.0959
Xe	−7232.1384	−7232.1211	−7232.1149	−7232.1388	−7232.1437	−7232.1558	−7232.1746	−7232.1985
Rn	−21 866.7722			−21 866.7729	−21 866.7797	−21 866.7964	−21 866.8225	−21 866.8568
AARE[b] (%)		0.0006	0.0009	0.0006	0.0008	0.0007	0.002	0.004

[a]This work with various values of μ (in a.u.$^{-1}$).
[b]Average of absolute relative error.

TABLE III. Comparison of the single-particle eigenvalue of the highest-energy occupied state ϵ_{HOS} (in hartree), calculated in various approximations for the noble-gas atoms.

					PW[a]				
	Exact	OEP [33]	KLI-OEP [29]	LDA	$\mu = 0.1$	$\mu = 0.2$	$\mu = 0.3$	$\mu = 0.4$	$\mu = 0.5$
He	−0.9180	−0.9176		−0.5170	−0.9173	−0.9163	−0.9152	−0.9142	−0.9133
Ne	−0.8504	−0.8486	−0.8507	−0.4431	−0.8488	−0.8458	−0.8429	−0.8408	−0.8398
Ar	−0.5910	−0.5885	−0.5908	−0.3338	−0.5893	−0.5869	−0.5859	−0.5868	−0.5890
Kr	−0.5241	−0.5212	−0.5239	−0.2999	−0.5223	−0.5199	−0.5197	−0.5217	−0.5249
Xe	−0.4573	−0.4543	−0.4573	−0.2657	−0.4553	−0.4524	−0.4543	−0.4573	−0.4608
Rn	−0.4280				−0.4260	−0.4243	−0.4258	−0.4292	−0.4327
AARE[b] (%)		0.4	0.03	44	0.3	0.7	0.7	0.5	0.7

[a]This work with various values of μ (in a.u.$^{-1}$).
[b]Average of absolute relative error.

methods can give very accurate energies as shown in Table II. The presented method with smaller values of μ also yields the total energy close to the exact value, while, for larger values of μ, it becomes worse than the OEP method. Interestingly, there seems to be a general tendency that the total energy by the presented method becomes lower as μ increases, while the OEP values are always higher than the exact value.

Finally, the question ought to be considered as to whether the present scheme can successfully reproduce the LR asymptotic tail of the exchange potential as expected. In Fig. 3, the calculated exchange potential of a helium atom is shown. The potential is defined here as the Coulomb potential generated by the exchange hole

$$U(\boldsymbol{r}) = -\frac{1}{2}\int \frac{\rho_X(\boldsymbol{r},\boldsymbol{r}')}{|\boldsymbol{r}-\boldsymbol{r}'|}d^3r'. \tag{40}$$

The LDA potential shows the well-known difference from the exact potential. For example, the asymptotic tail approaches to zero much faster than the exact $-1/r$ tail. The GGA potential not only shows no improvement in the tail, but also has an erroneous divergence at the origin. On the contrary, our method successfully reproduces the exact exchange potential. Note that the plotted potential (40) is different from the effective

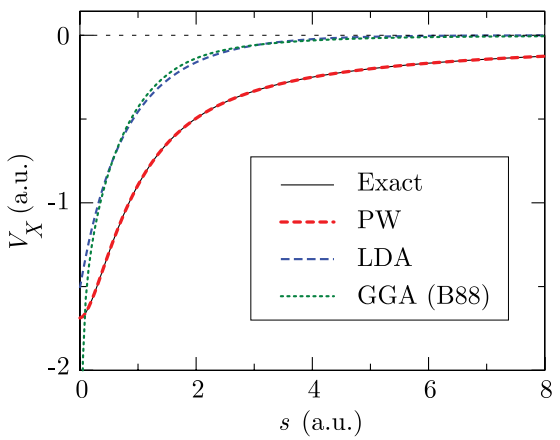

FIG. 3. (Color online) Exchange potential of a helium atom, calculated by the exact (solid line), LDA (dashed line), GGA [5] (dotted line), and the present (thick dashed line) method.

exchange potentials (34) appearing in the KS equations. To see that the effective potential (34) also has the correct shape, the single-particle eigenvalue of the highest-occupied state (HOS) is calculated and summarized in Table III. This serves as a simple but sensitive test as to whether the exchange potential has the correct asymptotic tail because it determines the tail of the HOS charge density. The LDA eigenvalue is much too high as commonly known, showing that it has a completely wrong potential at the asymptotic region. The presented method, on the other hand, can calculate reasonably accurate eigenvalues with error less than 1%.

We have shown that the presented method can reproduce accurate exact exchange energy and potential, and also that the degree of the approximation is systematically controlled by the separation parameter μ from the level of GGA ($\mu \sim 0.5$ a.u.$^{-1}$) to the level of OEP ($\mu \sim< 0.3$ a.u.$^{-1}$) or to even higher than that. This result would at least partly validate our ansatz that the LR part of the exchange energy can be well described by referring the corresponding SR part. The remaining question is how much the computation load can be reduced by the presented method with the typical values of μ. As a rough estimation, the effective range of the screening of $D^{\mathrm{erf}}(s)$ is given as

$$s_{\mathrm{eff}} = \frac{\int_0^\infty r^3 \mathrm{erfc}(\mu s)\,ds}{\int_0^\infty r^2 \mathrm{erfc}(\mu s)\,ds} = \frac{9\sqrt{\pi}}{16\mu}. \tag{41}$$

The values are $s_{\mathrm{eff}} = 5.3$, 1.8, and 1.1 Å at $\mu = 0.1$, 0.3, and 0.5 a.u.$^{-1}$, respectively. In actual calculations of the screened hybrid functional method [10], for example, the exchange energy contribution in a metallic carbon nanotube is reported to be converged at around 10 Å when the screening function $D^{\mathrm{erf}}(s)$ with $\mu = 0.15$ a.u.$^{-1}$ is used. We therefore expect that, by using the medium value $\mu = 0.3$ a.u.$^{-1}$, a reasonably accurate EXX can be calculated where the integrations are terminated at $s_{\mathrm{max}} \sim 5$ Å. A quantitative study is in progress where the presented method is implemented in a conventional DFT program and applied to molecules and solids.

IV. CONCLUSION

We have presented a scheme to calculate EXX with $O(N)$ computational scaling by truncating the numerical integrations, while the correct $-1/r$ asymptotic tail of the

exchange potential is well reproduced by an approximation to the tail of the exchange-hole density. The numerical calculations for the noble-gas atoms show that the presented scheme can provide accurate exchange energies. The method is based on a fundamental idea that the LR behavior of the interaction should somehow be extrapolated by referring the information obtained from the corresponding SR part due to the localized nature of 1-RDM of electrons. This idea should also be applicable for other methodologies based on 1-RDM, e.g., the reduced-density-matrix functional method and post HF methods. The low computational cost is advantageous especially for the large scale calculations and the present method can be immediately applied in the framework of the hybrid functional method or the range-separated EXX method. It would be, however, more challenging to search for a scheme with low computational cost based on the same idea for the correlation functional that is compatible with EXX.

ACKNOWLEDGMENTS

This work was partly supported by CREST-JST, the Next Generation Super Computing Project, Nanoscience Program, MEXT, Japan, and "Materials Design through Computics: Complex Correlation and Non-Equilibrium Dynamics" A Grant in Aid for Scientific Research on Innovative Areas MEXT, Japan.

[1] P. Hohenberg and W. Kohn, Phys. Rev. **136**, B864 (1964).
[2] W. Kohn and L. J. Sham, Phys. Rev. **140**, A1133 (1965).
[3] M. Levy, Proc. Natl. Acad. Sci. USA **76**, 6062 (1979).
[4] J. P. Perdew, K. Burke, and M. Ernzerhof, Phys. Rev. Lett. **77**, 3865 (1996).
[5] A. D. Becke, Phys. Rev. A **38**, 3098 (1988).
[6] J. P. Perdew and Y. Wang, Phys. Rev. B **45**, 13244 (1992).
[7] A. D. Becke, J. Chem. Phys. **98**, 1372 (1993).
[8] J. P. Perdew, M. Ernzerhof, and K. Burke, J. Chem. Phys. **105**, 9982 (1996).
[9] C. Adamo and V. Barone, J. Chem. Phys. **110**, 6158 (1999).
[10] J. Heyd, G. E. Scuseria, and M. Ernzerhof, J. Chem. Phys. **118**, 8207 (2003).
[11] D. M. Bylander and L. Kleinman, Phys. Rev. B **41**, 7868 (1990).
[12] A. Seidl, A. Görling, P. Vogl, J. A. Majewski, and M. Levy, Phys. Rev. B **53**, 3764 (1996).
[13] H. Iikura, T. Tsuneda, T. Yanai, and K. Hirao, J. Chem. Phys. **115**, 3540 (2001).
[14] S. J. Clark and J. Robertson, Phys. Rev. B **82**, 085208 (2010).
[15] M. Toyoda and T. Ozaki, J. Chem. Phys **130**, 124114 (2009).
[16] T. Leininger, H. Stoll, H.-J. Werner, and A. Savin, Chem. Phys. Lett. **275**, 151 (1997).
[17] J. Toulouse, F. Colonna, and A. Savin, Phys. Rev. A **70**, 062505 (2004).
[18] J. Toulouse, P. Gori-Giorgi, and A. Savin, Int. J. Quantum Chem. **106**, 2026 (2006).
[19] W. Kohn, Phys. Rev. Lett. **76**, 3168 (1996).
[20] S. Goedecker, Rev. Mod. Phys. **71**, 1085 (1999).
[21] S. Ismail-Beigi and T. A. Arias, Phys. Rev. Lett. **82**, 2127 (1999).
[22] S. Goedecker, Phys. Rev. B **58**, 3501 (1998).
[23] W. A. Harrison, *Solid State Theory* (McGraw-Hill, New York, 1970).
[24] A. D. Becke and M. R. Roussel, Phys. Rev. A **39**, 3761 (1989).
[25] S. H. H. Taketa and K. O-ohata, J. Phys. Soc. Jpn. **21**, 2313 (1966).
[26] T. Ozaki and M. Toyoda, Comput. Phys. Commun. (in press).
[27] The smearing shows the limitation of the model function Eq. (12) not to have a multiple-peak structure because it is derived from a nodeless 1*s* orbital.
[28] Y. Wang, J. P. Perdew, J. A. Chevary, L. D. Macdonald, and S. H. Vosko, Phys. Rev. A **41**, 78 (1990).
[29] J. B. Krieger, Y. Li, and G. J. Iafrate, Phys. Rev. A **45**, 101 (1992).
[30] R. T. Sharp and G. K. Horton, Phys. Rev. **90**, 317 (1953).
[31] J. D. Talman and W. F. Shadwick, Phys. Rev. A **14**, 36 (1976).
[32] R. K. Nesbet and R. Colle, Phys. Rev. A **61**, 012503 (1999).
[33] Y. Li, J. B. Krieger, J. A. Chevary, and S. H. Vosko, Phys. Rev. A **43**, 5121 (1991).